ACS APPLIED MATERIALS & INTERFACES

Research Article

www.acsami.org

Block Copolymer Hollow Fiber Membranes with Catalytic Activity and pH-Response

Roland Hilke,[†] Neelakanda Pradeep,[†] Poornima Madhavan,[‡] Ulla Vainio,[⊥] Ali Reza Behzad,[§] Rachid Sougrat,[§] Suzana P. Nunes,[‡] and Klaus-Viktor Peinemann*,[†]

[†]Advanced Membranes and Porous Materials Center, [‡]Water Desalination and Reuse Center, and [§]Imaging and Characterization Lab, King Abdullah University of Science and Technology (KAUST), Thuwal 23955-6900, Saudi Arabia

[⊥]Photon Science, Deutsches Elektronen Synchrotron (DESY), Notkestr. 85, 22607 Hamburg, Germany

Supporting Information

ABSTRACT: We fabricated block copolymer hollow fiber membranes with self-assembled, shell-side, uniform pore structures. The fibers in these membranes combined pores able to respond to pH and acting as chemical gates that opened above pH 4, and catalytic activity, achieved by the incorporation of gold nanoparticles. We used a dry/wet spinning process to produce the asymmetric hollow fibers and determined the conditions under which the hollow fibers were optimized to create the desired pore morphology and the necessary mechanical stability. To induce ordered micelle assembly in the doped solution, we identified an ideal solvent mixture as confirmed by small-angle X-ray scattering. We then reduced *p*-nitrophenol with a gold-loaded fiber to confirm the catalytic performance of the membranes.

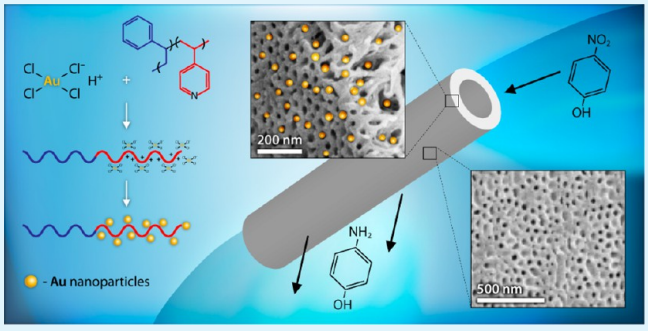

KEYWORDS: *block copolymer, self-assembly, membrane, hollow fiber, filtration, catalysis*

INTRODUCTION

We recently demonstrated that isoporous membranes can be obtained by combining block copolymer micelle assemblies with phase separation by solution casting and immersion in water.[1−3] One advantage of this method is the possibility of exploiting the unique versatility of block copolymers for morphological design, a claim that many groups have made,[4−8] to improve membranes used by industry on the large scale. We are now able to prepare isoporous block copolymer flat-sheet membranes continuously by using nonwoven substrates as supports.[3] For many applications, such as artificial kidneys, membrane bioreactors, contactors, or specific cases of gas separation, however, hollow fiber membranes rather than flat sheets are preferred,[9,10] because they have higher surface-to-volume ratios, which allow their integration into compact modules. No support is necessary for hollow fibers.

The principle of fabricating hollow fibers is simple, and we have explored the use of many materials and applications for these membranes. The polymer (dope) solution is pressed through a spinneret and collected in a rotating immersion bath filled with water (Figure S1, Supporting Information). By simultaneously pressing water or other nonsolvent mixtures (bore fluid) from the center of the spinneret, a continuous hollow fiber can be manufactured. The big challenge is to adapt the casting solutions and production conditions to produce fibers with high dimensional stability, while maintaining the isoporous surface structure. We note that the complete formation of the membrane structure must be finished in less than 5 s. This short time is determined by the spinning speed (typically 5 m/min), the air gap length (14 cm in most of our experiments), and the very fast precipitation step. Whereas these conditions are well established for routine hollow fiber spinning, our challenge is that a highly ordered, self-assembled fiber top layer must also be formed in this short period. This is possible only because we preorder the micelles in the polymer solution. A new solvent mixture was also needed to produce the hollow fibers, and the manufacturing conditions had to be adapted to produce mechanically stable systems that would withstand regular operating conditions.

We recently demonstrated that membranes with exceptionally regular pore sizes and with the ability to respond to pH can be used for separation of similarly sized proteins.[11] Here, we look beyond separation to describe the catalytic capabilities of isoporous hollow fiber membranes that incorporate colloidal gold. The inclusion of gold nanoparticles in block copolymers has been previously reported for the formation of micelles, vesicles, and nanofibers with applications in biotechnology and biomedicine, cellular imaging, and nanowires.[12−15] Gold catalysis is relevant to the reduction of highly toxic 4-

Received: April 2, 2013
Accepted: July 18, 2013
Published: July 18, 2013

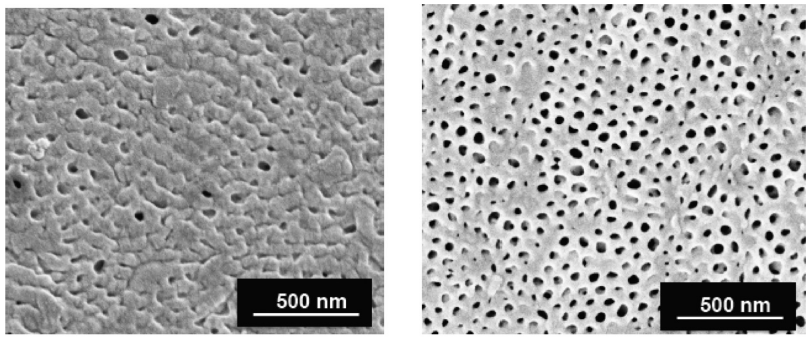

(a) (b)

Figure 1. FESEM micrographs of the outer surfaces of the hollow fiber membranes prepared with a 16 wt % copolymer solution in DMF/THF/dioxane with a dope flow of (a) 6 and (b) 3.4 mL/min.

nitrophenol to 4-aminophenol,[16,17] which we used as our model reaction to test our novel membranes.

EXPERIMENTAL SECTION

Materials. Polystyrene-*b*-poly vinyl pyridine block copolymer samples (number P9828-S4VP (PS-*b*-P4VP, 175 000-*b*-65 000)) were purchased from Polymer Source, Inc., Canada. 1,4-Dioxane, acetone, dimethylformamide (DMF), nitric acid, sodium hydroxide, gold tetra chloride, and sodium citrate were supplied by Sigma Aldrich, and tetrahydrofuran (THF) was supplied by Fischer Scientific. Single wall carbon nanotubes were supplied by Sigma Aldrich.

Membrane Preparation. Flat-sheet membranes were prepared for comparison. Dope solution 1 was prepared by dissolving 16 wt % block copolymer in a mixture of DMF, THF, and 1,4-dioxane of equal weight proportions. The casting solution was stirred overnight at room temperature. When the solution was free from air bubbles, it was cast using a doctor blade with a gap of 200 μm. The polymer solutions were cast on a glass plate and precipitated in deionized water. Finally, the membranes were rinsed with water and dried at 22 °C.

We used ternary solvent mixtures for preparation of the spinning dopes. The spinning solution, which resulted in the most uniform pore structure consisted of 22 wt % block copolymer, 42 wt % dioxane, 20 wt % DMF, and 16 wt % acetone. Table S1 (Supporting Information) shows the composition of all tested spinning dopes.

The hollow fiber membranes were produced with a small laboratory spinning apparatus as shown in Supporting Information Figure S1. Both the bore fluid and polymer flow were carefully controlled. The bore fluid was pumped by a HPLC pump (Knauer Scientific Instruments, Germany). A nitrogen pressure-induced flow controlled by a digital thermal mass flow meter (Bronkhorst, El-flow, Germany) regulated the flow of the dope.

Deionized water at a temperature of 22 °C was used for the precipitation bath and as the bore fluid. The nascent fiber entered an air gap between the spinneret and the precipitation bath. The moisture in the air gap was regulated by a laminar flow of nitrogen with a relative humidity of 20% at 22 °C into the air gap housing. Finally, the fibers were rinsed for at least two days in deionized water that was renewed daily and then air-dried at 22 °C.

We used two methods to deposit gold nanoparticles on the outer surface of the hollow fiber membranes. In one set of experiments, we first prepared the gold nanoparticles as a dispersion, which was then filtered through the hollow fiber membranes (details in the Supporting Information). In a second set of experiments, we filtered a 1 wt % gold chloride solution through the fibers. The adsorbed gold ions were then reduced to elementary gold by pumping a 0.05 M sodium citrate solution through the hollow fiber membranes (details in the Supporting Information).

We used the model reaction of the reduction of *p*-nitrophenol[16] to confirm the catalytic activity of the hollow fibers after incorporation with gold. The absorbance of the solution in contact with the hollow fibers was measured over time. An absorbance peak at 400 nm is characteristic of *p*-nitrophenol. As the reaction takes place, the peak gradually decreased.

Flux Measurement. Flux through the flat sheet membranes was measured with an Amicon filtration cell at a pressure of 1 bar. The pH of the feed solution was adjusted by adding nitric acid or sodium hydroxide. Small single fiber modules each containing a fiber about 9 cm in length were used for the flux measurements. A filtration setup like that shown in Figure S2 (Supporting Information) was used. pH-Adjusted solutions were pumped through the hollow fiber modules by a roller pump (Heidolph, Pumpdrive 5001, Germany), and the pressure was monitored by a digital pressure sensor (Greisinger Electronic, GDH13AN, Germany). A needle valve regulated the pressure.

Characterization. The morphology of the membranes was characterized by a field emission scanning electron microscope (FESEM). The membrane surfaces were imaged with a Nova Nano 630 microscope using a voltage of 5 kV. Prior to the imaging, the samples were sputtered with Pt using a K575X Emitech sputter coater. Secondary and backscattered detectors were also used.

Further, the membranes were cut in a LEICA EM UC6 cryo-ultramicrotome after being embedded in a low viscosity resin and imaged in a Titan FEI transmission electron microscope (TEM) at 300 kV. For clarity in some of the images, the membrane slices were stained with methyl iodide vapor for 4 h before imaging.

Casting solutions with different copolymer concentrations and a mixture of DMF/dioxane/acetone were investigated by small-angle X-ray scattering (SAXS) with the B1 beamline of the DORIS III, HASYLAB of the *Deutsches Elektronen-Synchrotron* (DESY) in Hamburg, Germany. The solution was placed into 2 mm diameter quartz capillaries by using a syringe and sealed with epoxy glue. The experiments were performed at $P = 10^{-4}$ mbar using a single-photon counting PILATUS 1 M detector (Dectris) placed 3.6 m behind the sample. The X-ray wavelength was 1.764 Å, with a photon flux of $\sim 10^8$ photons/s on the sample. The scattering vector magnitude, q, is defined as $q = (4\pi/\lambda)\sin\theta$, where θ is half of the scattering angle.

RESULTS AND DISCUSSION

Surface Characterization. Although the formation of isoporous flat-sheet membranes has been demonstrated before with DMF/THF[18] and DMF/THF/dioxane,[2] we had to optimize the system to produce hollow fibers with adequate properties and sufficient stability for ultrafiltration.

Our preliminary experiments[19] to develop isoporous PS-*b*-P4VP block copolymer hollow fibers were conducted with 16 wt % DMF/THF/dioxane and DMF/THF. The rates of the polymer (dope) solution flow and the bore flow (water) were 6 and 1.2 mL/min, respectively. The morphology of the outer surface of the hollow fibers produced at a flow rate of 6 mL/min is shown in the FESEM image in Figure 1a where it is clear that the pores are mostly closed and the porosity is low. We

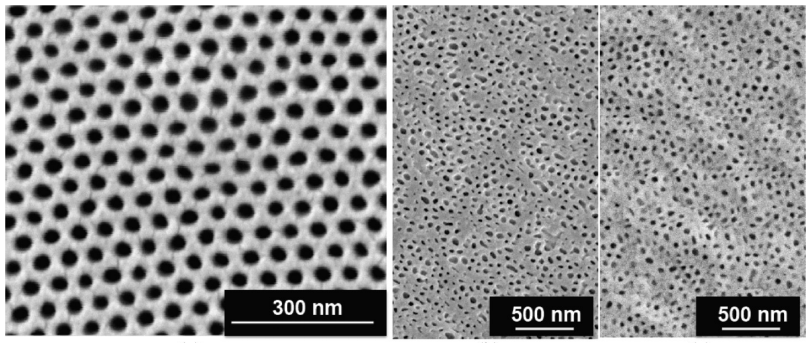

Figure 2. FESEM micrographs of the outer surface of (a) a flat-sheet membrane and (b) a hollow fiber made from 22 wt % copolymer solutions in DMF/acetone/dioxane. (c) Outer surface of a hollow fiber prepared from the same solution with the addition of 0.08 wt % carbon nanotubes.

surmised that the poor surface morphology of this hollow fiber membrane was caused by the shear rate in the spinneret. We recently demonstrated by SAXS and dissipative particle dynamics simulation[20] that PS-*b*-P4VP form micelles in the concentration range used for membrane manufacturing. The micelles assemble later to form the regular pores. The order in solution is fragile and can be disturbed under high shear rate. Viscosity measurements for the casting solution show a shear thinning behavior (see Figure S3 measured for a similar system, 15 wt % PS-*b*-P4VP in DMF/dioxane, as Supporting Information). This indicates that under shear the ordered micelle assembly might be disrupted and the spherical micelles loosing the shape . The structure is then affected. An extreme result of this alignment can be seen in Figure 4 (SEM image) for the internal part of the fibers. It should be noted that on the bore side we have an immediate contact with the inner coagulant without any evaporation. Since for our system an evaporation time is relevant for the formation of the iso-porous skin layer, we cannot get an ordered structure on the hollow fiber inside.

We found that it is possible to decrease the shear rate with either a larger annulus in the spinneret or a lower volume flow of polymer solution. We used the lowest possible dope solution flow in the available setup, which we found to be 3.4 mL/min. The improved structure of the outer surface as shown in the SEM image in Figure 1b is the result of the lower shear rate, which allowed us to produce isoporous hollow fibers based on block copolymers.[19] A similar attempt using DMF/THF as the solvent mixture was recently reported by Radjabian et al.[21] No uniform pore size could be obtained although the crucial influence of the shear rate on the pore structure was identified. The surface structure obtained here with DMF/THF/dioxane using a dope flow rate of 3.4 mL/min is certainly more uniform. This observation also confirms our previous findings for flat sheet membranes with dioxane as an additional solvent.[2] However, the fibers produced with solutions containing both DMF and THF are not flexible and can easily break, features that are not acceptable for integration of the fibers into modules or even lab-scale operations. Two methods were investigated to increase the mechanical stability of the fibers: (i) increasing the polymer concentration and (ii) adding carbon nanotubes to the mixture. When we increased the polymer concentration in the DMF/THF/dioxane solvent system, the surface morphology was less ordered, even in the flat-sheet membranes, which we prepared for comparison. A high polymer concentration can also cause a reduction in the water permeance, a property relevant to many practical applications.

Using the values of the solubility parameters of each polymer block and solvent, we discussed in a previous paper why a ternary mixture of DMF, THF, and dioxane favors the formation of an isoporous self-assembled membrane top-layer of flat sheet membranes.[2] For the hollow fiber membranes we obtained better results when THF was replaced by acetone. Acetone has a higher evaporation rate than THF. The relative evaporation rate of acetone is 14.4 compared to 8.0 for THF (*n*-butylacetate = 1). Evaporation of solvent from the film surface prior to precipitation is important for the micelle self-assembly and structure formation as shown in our previous work.[1−3,18] The standard dry-wet spinning process allows only a short evaporation time, which is determined by the distance spinneret to water bath and the spinning speed. The fast acetone evaporation enables this reduction in evaporation time. The membranes shown in Figure 2 were prepared from a casting dope with 22 wt % polymer dissolved in a DMF/acetone/dioxane solvent mixture. In addition, our solvent mixture must be selective for the polyvinyl pyridine block in order to create micelles with a PVP shell. By taking in account the dispersive, polar, and H-bond contributions to solubility parameters of both copolymer blocks as well as all solvent involved (Table S3, Supporting Information), acetone stimulates the micelle formation even more than THF with a PS core which can be hardly swollen by the solvent.

Figure 2a shows the surface of a flat sheet membrane and Figure 2b the outer surface of a hollow fiber membrane. Figure 2c shows the outer surface of a hollow fiber membrane which contains 0.08 wt % carbon nanotubes. We added the carbon nanotubes to improve the mechanical stability of the fibers. Only qualitative testing was performed to evaluate the mechanical stability. Whereas the fibers spun from a DMF/THF/dioxane solution were quite brittle when in a dry state, the fibers manufactured from DMF/acetone/dioxane were still flexible.

SAXS Characterization. We recently demonstrated[22] that controlling the micelle assembly of block copolymer in solution is essential to the final pore morphology of the membrane. We therefore investigated the order of the PS-*b*-P4VP in DMF/dioxane/acetone solutions by small-angle X-ray scattering. The results for different copolymer concentrations are shown in Figure 3. Scattering patterns confirmed the occurrence of a two-dimensional hexagonal order with peak positions compared to the first peak following the ratio 1, $\sqrt{3}$, and 2 in copolymer concentrations higher than 20 wt %, which was in

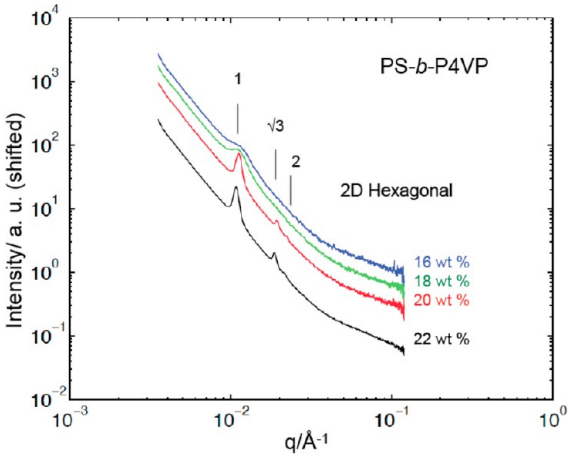

Figure 3. Small-angle X-ray scattering of PS-*b*-P4VP copolymer solutions in DMF/dioxane/acetone.

optimized range for hollow fiber production. With copolymer concentrations lower than 20 wt %, we observed only the first peak practically at the same position. This measurement confirms that the needed micelle assembly is incipient before spinning. The ordered structure is frozen when the hollow fiber is immersed in water.

Process Optimization. The process of making hollow fiber membranes was further optimized with respect to the air gap humidity and length of the membrane and with respect to the bore fluid composition and flow. As noted above, we fixed the dope flow at 3.4 mL/min. A bore flow of 2.4 mL/min produced the best results with thin-walled round fibers consistently produced. For our setup, the minimal fiber speed for a continuously spun fiber was 7 cm/s. We obtained good results with an air gap of 14 cm and a relative humidity of 20%. The resulting evaporation time of 2 s was short compared with the 10 s evaporation time for the flat sheet membranes. This might be one reason for the prevalence of less uniform pores on the surface of the hollow fibers. We could achieve a porous sponge-like structure without any macrovoids, as shown in Figure 4, with a well-ordered, highly porous outer surface.

Hollow fibers prepared using water as the bore fluid had dense internal surfaces (Figure S4, Supporting Information), which led to low water permeance. By adding 33 wt % DMF to the bore fluid, we could obtain a more open internal structure, as shown in Figure 4. Moreover, greater than 3-fold higher water permeance was achieved by the addition of DMF to the bore fluid (Figure 5). The addition of solvent to the bore coagulant slows down the outflow of solvent from the spinning dope and leads to a delayed demixing and phase separation. The result is a more open inner layer of the hollow fiber. The addition of solvent to the precipitation bath is a well-known method for increasing the porosity of the skin layer.[23,24]

Hollow Fibers with pH Response. We showed earlier that asymmetric flat sheet membranes made from PS-*b*-P4VP exhibited a strong pH response.[1,11] We have now found that PS-*b*-P4VP hollow fiber membranes behave similarly. The water permeance of the hollow fiber membranes was very low when the pH was below 2, whereas a steep but reversible

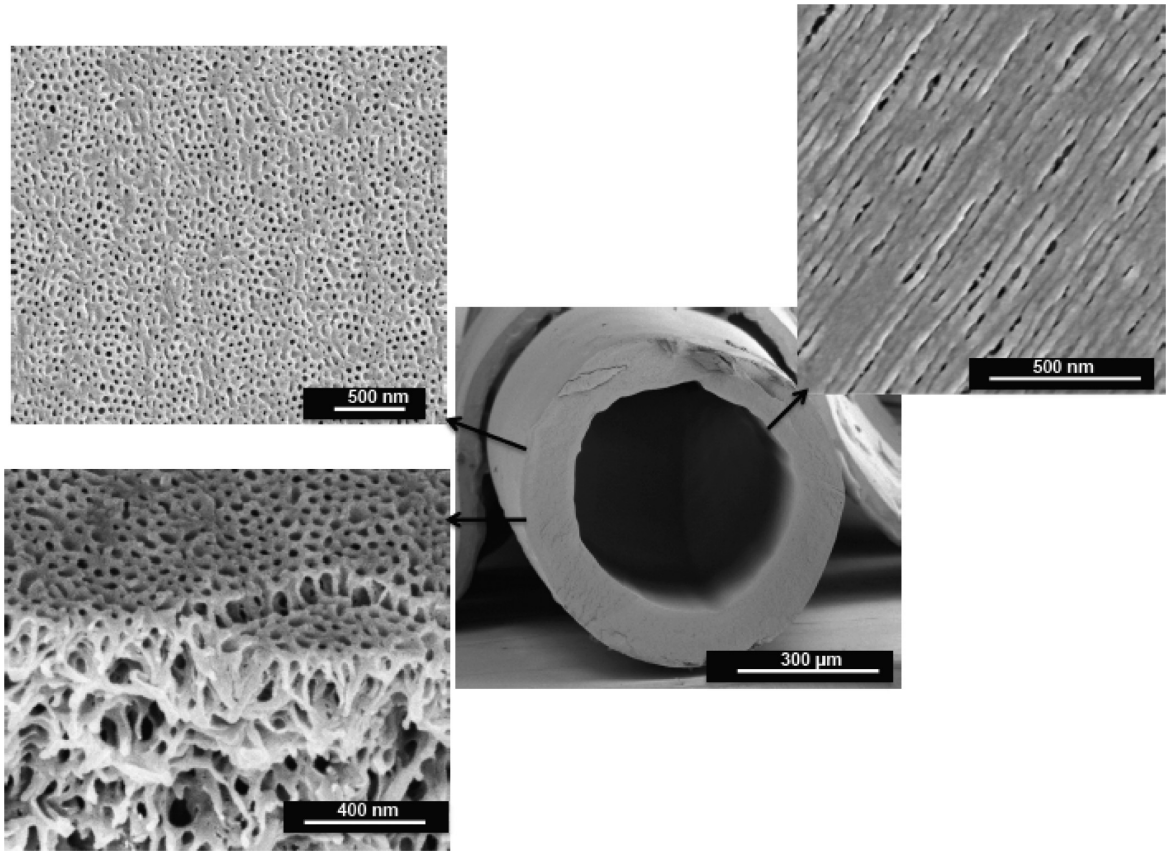

Figure 4. FESEM images of the surface morphology of optimized hollow fibers made from 22 wt % PS-*b*-P4VP in a DMF/acetone/dioxane solvent system spun with water/DMF bore fluid.

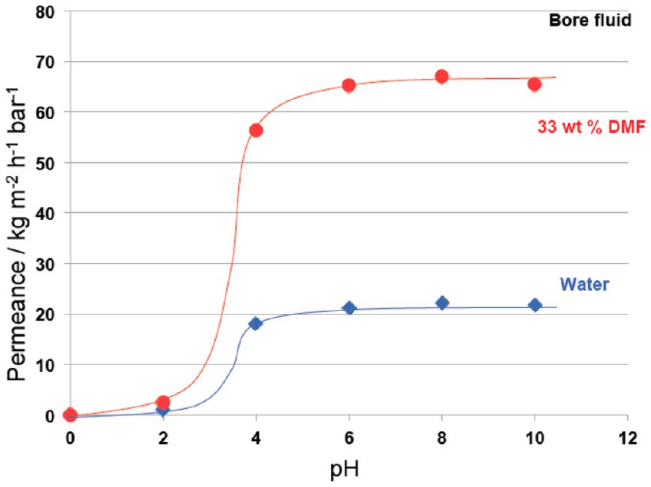

Figure 5. Water permeance of hollow fibers prepared from 22 wt % PS-*b*-P4VP in a DMF/acetone/dioxane solvent system using water or water/33 wt % DMF as the bore fluid (feed pressure: 1.2 bar).

increase in water flux occurred when the pH was around 4 (Figure 5). When we switched the pH from low values to pH larger 7, the original high water fluxes could be recovered. The water flux through the fibers prepared with pure water as bore fluid is small compared with the flux of the fibers manufactured with a water/DMF mixture as bore fluid. The reason is the tighter structure of the inner fiber surface (see Figure S4, Supporting Information). We calculated in our previous publication[1] the change of pore size with pH using the Hagen–Poiseuille equation. The calculated pore diameter for the flat sheet membrane was around 19 nm at pH 7 and 5 nm at pH 2. We assume a similar ratio here, but the application of Hagen–Poiseuille's is difficult, because the resistance of the inner part of the fiber wall and also the inner skin influences the flux. The pH response of the hollow fiber membranes would be important in biomedical applications because they can be integrated into very small devices, while maintaining the reversible pH response.

Hollow Fibers with Catalytically Active Gold Nanoparticles. Our two methods, either depositing preformed colloidal gold or reducing the gold ions after adsorption, resulted in the deposition of nanosized gold particles on the outer surface of the fibers. The particles were preferentially placed in the pyridine coronas and could be detected by electron microscopy (Figures 6 and 7).

The catalytic activity was tested using a small one-fiber module (fiber length 9.9 cm, fiber diameter 694 μm, effective area 2.16 cm^2). A 100 mL portion of a solution containing 1.39 mg nitrophenol and 37.83 mg sodium borohydride as a reducing agent was pumped under a pressure of 1.5 bar through the hollow fiber module. About 0.5 mL of the solution was collected as the permeate after 21 h. Figure 8 shows the nitrophenol peak at 400 nm of both the feed and the permeate. The nitrophenol concentration in the permeate was reduced from 0.1 to 0.023 mM due to reduction to aminophenol. The calibration curve for the determination of the nitrophenol concentration can be found in the Supporting Information. (Figure S5).

Conclusion. Here, we demonstrated for the first time the production of PS-*b*-P4VP hollow fibers with narrow pore size distributions and pH response. We found that a short evaporation time of 2 s was sufficient for the formation of the self-assembled, shell-side skin layer. We confirmed the preassembly of the block copolymer micelles in the casting solution, which is requisite for the fast self-assembly process, by small-angle X-ray scattering. Fibers spun from a DMF/dioxane/acetone dope were flexible when in dry state, whereas fibers made from a DMF/dioxane/THF solution were brittle.

We showed that the hollow fiber pores acted as pH-responsive gates with a large step in permeance around pH 4. Additionally, we deposited gold nanoparticles on the outer fiber surface and demonstrated the catalytic activity of the gold nanoparticle-enhanced hollow fiber membranes by the reduction of nitrophenol to aminophenol.

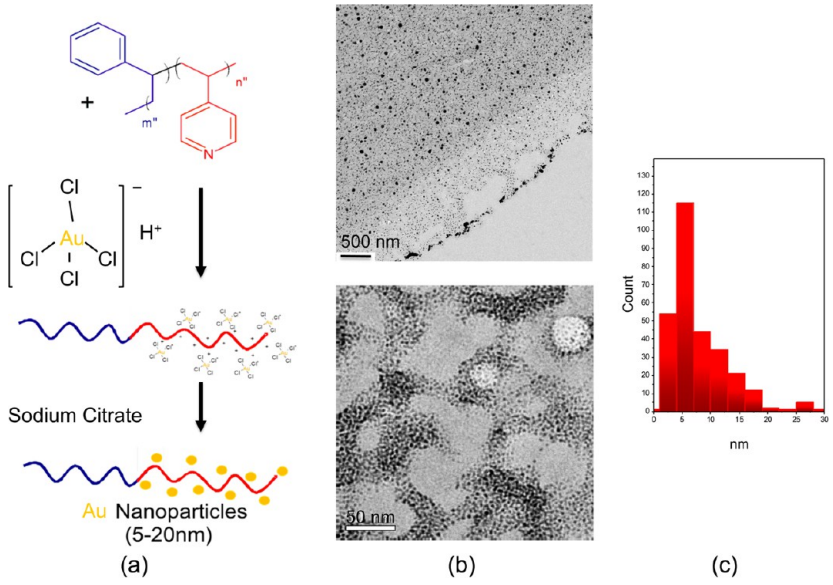

Figure 6. (a) Preparation of catalytic membranes by treatment with gold salts followed by reduction with sodium citrate. (b) TEM image of a hollow fiber membrane cross-section with gold nanoparticles. (c) Size distribution of the gold nanoparticles around 5 nm.

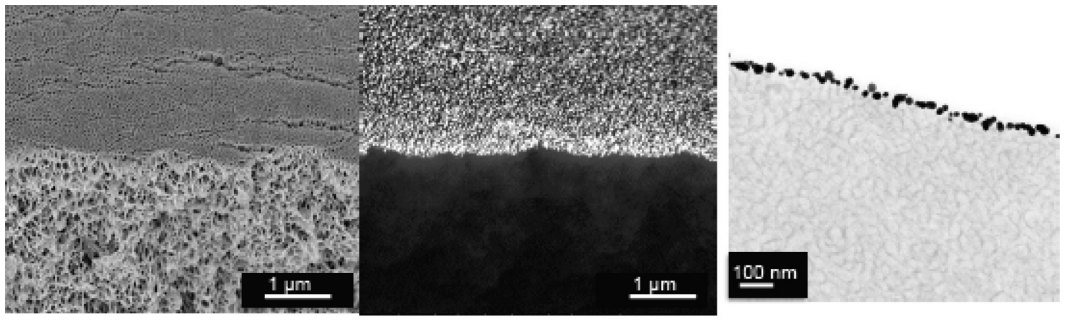

Figure 7. Hollow fibers with gold nanoparticles. FESEM images of the (a) secondary and (b) backscattering electrons. (c) TEM image of a cross-section of a fiber.

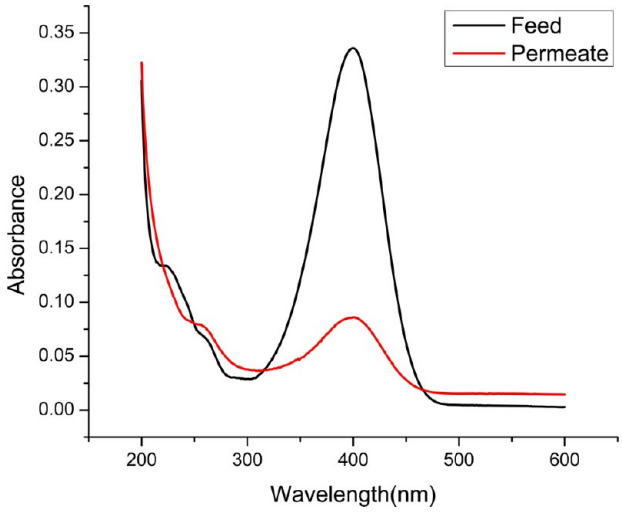

Figure 8. Reduction of *p*-nitrophenol to *p*-aminophenol catalyzed by gold nanoparticles and followed by UV absorbance measurements.

■ ASSOCIATED CONTENT

Supporting Information

Schematic of hollow fiber spinning and flux measurement setup, preparation of gold nanoparticles, SEM picture of inner hollow fiber surface, table with solubility parameters for solvents and polymer segments, table with manufacturing parameters for all hollow fibers, description of nitrophenol analysis. This material is available free of charge via the Internet at http://pubs.acs.org.

■ AUTHOR INFORMATION

Corresponding Author

*Tel.: +966 544700053. E-mail: klausviktor.peinemann@kaust.edu.sa.

Notes

The authors declare no competing financial interest.

■ ACKNOWLEDGMENTS

Portions of this research were carried out at the light source DORIS III at DESY, a member of the Helmholtz Association (HGF). The authors thank Prof. Valerie Caps (Catalysis Center, KAUST) for advice for preparation of the gold nanoparticles and Dr. Wolfgang Albrecht (retired, Berlin) for helpful discussion of the hollow fiber spinning process.

■ REFERENCES

(1) Nunes, S. P.; Behzad, A. R.; Hooghan, B.; Sougrat, R.; Karunakaran, M.; Pradeep, N.; Vainio, U.; Peinemann, K.-V. *ACS Nano* **2011**, *5*, 3516−3522.
(2) Nunes, S. P.; Karunakaran, M.; Pradeep, N.; He, H.; Behzad, A. R.; Hooghan, B.; Sougrat, R.; Peinemann, K.-V. *Langmuir* **2011**, *27*, 10184−10190.
(3) Nunes, S. P.; Sougrat, R.; Hooghan, B.; Anjum, D. H.; Behzad, A. R.; Zhao, L.; Pradeep, N.; Pinnau, I.; Vainio, U.; Peinemann, K.-V. *Macromolecules* **2010**, *43*, 8079−8085.
(4) Bates, F. S.; Hillmyer, M. A.; Lodge, T. P.; Bates, C. M.; Delaney, K. T.; Fredrickson, G. H. *Science* **2012**, *434*, 440.
(5) Park, C.; Yoon, J.; Thomas, E. L. *Polymer* **2003**, *44*, 6725−6760.
(6) Park, S.; Lee, D. H.; Xu, J.; Kim, B.; Hong, S. W.; Jeong, U.; Xu, T.; Russell, T. P. *Science* **2009**, *323*, 1030.
(7) Ruzette, A. V.; Leibler, L. *Nat. Mat.* **2005**, *4*, 19−31.
(8) Mai, Y.; Eisenberg, A. *Chem. Soc. Rev.* **2012**, *41*, 5969−5985.
(9) Kneifel, K.; Nowak, S.; Albrecht, W.; Hilke, R.; Just, R.; Peinemann, K.-V. *J. Membr. Sci.* **2006**, *276*, 241−251.
(10) Kneifel, K.; Peinemann, K.-V. *J. Membr. Sci.* **1992**, *65*, 295−307.
(11) Qiu, X.; Yu, H.; Karunakaran, M.; Pradeep; Nunes, S. P.; Peinemann, K.-V. *ACS Nano* **2013**, *7*, 768−776.
(12) Mai, Y.; Eisenberg, A. *Acc. Chem. Res.* **2012**, *45*, 1657−1666.
(13) Nandan, B.; Stamm, M.; Horechyy, A.; Chen, H. L.; Srivastava, R.; Pal, J.; Sanwaria, S. *J. Mater. Chem.* **2012**, *22*, 25102−25107.
(14) Kao, J.; Thorkelsson, K.; Bai, P.; Rancatore, B. J.; Xu, T. *Chem. Soc. Rev.* **2013**, *42*, 2654−2678.
(15) Daniel, M. C.; Astruc, D. *Chem. Rev.* **2004**, *104*, 293.
(16) Chen, X.; Zhao, D.; An, Y.; Zhang, Z.; Cheng, J.; Wang, B.; Shi, L. *J. Colloid Interface Sci.* **2008**, *322*, 414−420.
(17) Kuroda, K.; Ishida, T.; Haruta, M. *J. Mol. Catal. A: Chem.* **2009**, *298*, 7−11.
(18) Peinemann, K.-V.; Abetz, V.; Simon, P. F. W. *Nat. Mat.* **2007**, *6*, 992−996.
(19) Peinemann, K.-V. Self-assembled block copolymer membranes with high water flux and selectivity. In *IUPAC MACRO World Polymer Congress*, Blacksburg, VA, June 24−29, 2012.
(20) Marques, D. S.; Vainio, U.; Chapparo, N. M.; Calo, V. N.; Behzad, A. R.; Pitera, J. W.; Peinemann, K.-V.; Nunes, S. P. *Soft Matter* **2013**, *9*, 5557−5564.
(21) Radjabian, M.; Koll, J.; Buhr, K.; Handge, U. A.; Abetz, V. *Polymer* **2013**, *54*, 1803−1812.
(22) Dorin, R. M.; Marques, D. S.; Sai, H.; Vainio, U.; Phillip, W. A.; Peinemann, K.-V.; Nunes, S. P.; Wiesner, U. *ACS Macro Lett.* **2012**, *1*, 614−617.
(23) Koops, H.; Nolten, J. A. M.; Mulder, H. V.; Smolders, C. A. *J. Appl. Polym. Sci.* **1994**, *54*, 385−404.
(24) Santoso, Y. E.; Chung, T. S.; Wang, K. Y.; Weber, M. *J. Membr. Sci.* **2006**, *282*, 383−392.